Estimating the soil temperature profile from a single depth observation: A simple empirical heatflow solution

T. R. H. Holmes,[1] M. Owe,[2] R. A. M. De Jeu,[1] and H. Kooi[1]

Received 26 February 2007; revised 7 September 2007; accepted 29 October 2007; published 6 February 2008.

[1] Two field data sets are used to model near-surface soil temperature profiles in a bare soil. It is shown that the commonly used solutions to the heat flow equations by Van Wijk perform well when applied at deeper soil layers, but result in large errors when applied to near surface layers, where more extreme variations in temperature occur. The reason for this is that these approaches do not consider heat sources or sinks below the surface. This paper proposes a new approach for modeling the surface soil temperature profiles from a single observation depth. This approach consists of two parts: 1) modeling an instantaneous ground flux profile based on net radiation and the ground heat flux at 5 cm depth; and 2) use of this ground heat flux profile to extrapolate a single temperature observation to a complete surface temperature profile. The new model is validated under different field and weather conditions showing low RMS errors of 1–3 K for wet to dry conditions. Finally, the proposed model is tested under limitations in input data that are associated with remote sensing applications. It is shown that these limitations result in only small increases in the overall error. This approach may be useful for satellite-based global energy balance applications.

Citation: Holmes, T. R. H., M. Owe, R. A. M. De Jeu, and H. Kooi (2008), Estimating the soil temperature profile from a single depth observation: A simple empirical heatflow solution, *Water Resour. Res.*, *44*, W02412, doi:10.1029/2007WR005994.

1. Introduction

[2] Soil temperature is an important parameter in energy balance applications such as land surface modeling, numerical weather forecasting, and climate prediction. It is also important in radiative transfer applications, such as in the retrieval of land surface properties with satellite sensors, and especially in the retrieval of surface soil moisture with microwave sensors. Unlike other hydro-meteorological parameters such as air temperature and precipitation, soil temperature is rarely measured on a regular basis at meteorological and climate stations. Although some long-term measuring stations have been established (e.g., the Natural Resources Conservation Service Soil Climate Analysis Network), most historical soil temperature databases have been compiled from various field experiments, which are usually limited in both temporal and spatial coverage. Furthermore, the depth at which soil temperature is collected typically varies according to the specific application for which the measurement campaign was designed.

[3] Space-based remote sensing offers potentially the greatest single contribution to large-scale monitoring of the Earth's surface. If properly utilized, satellite systems can offer the spatial, temporal, and spectral resolution necessary for consistent and continuous coverage of the whole Earth environment and its surrounding atmosphere. Remote sensing technology is central to the integration of the many interrelated but highly variable point scale phenomena to more useful, regionally-oriented land surface processes. Land surface temperature may be derived by several remote sensing methods, including infrared and microwave techniques. While these techniques have shown to provide relatively accurate estimates, the measurements represent the temperature only at the very near surface. However, soil temperature gradients may be especially steep near the surface, and reasonable approximations of the near-surface temperature profile are important for a variety of modeling applications. Unfortunately, many of the parameterizations required in the application of more complex heat flow models are not available at global scales, and less complex approaches are often appropriate.

[4] Many models have been developed to extend limited temperature data [*Van Wijk and De Vries*, 1963; *Camillo*, 1989; *Cuaraglia et al.*, 2001; *Elias et al.*, 2004]. When properly implemented, these models can be used to extrapolate soil profile temperatures with reasonable accuracy from a single subsurface measurement. *Van Wijk and De Vries* [1963] fitted sine waves with diurnal and seasonal periods to the observed temperature cycles at two depths. The amplitude of these temperature oscillations decreases exponentially with depth. Others have built on Van Wijk's Fourier series to broaden the scope of that model. *Camillo* [1989] combined the Fourier series with a simple model of time dependent surface soil heat flux. This model was fitted to observations to derive five model parameters, but this makes it difficult to apply on a broader scale. More recently, *Elias et al.* [2004] improved on the Van Wijk model By introducing a correction for the temporal variation of daily amplitude. This addition makes the model better suited for inter-seasonal timescales. A different approach was used by *Cuaraglia et al.* [2001], who used electrical modeling to

[1] VU University Amsterdam, Dept. of Geo-Environmental Sciences, Amsterdam, The Netherlands.
[2] NASA GSFC, Hydrological Sciences Branch, Greenbelt, Maryland, USA.

0043-1397/08/2007WR005994$09.00

predict temperature and heat flow at one depth from solar radiation.

[5] However, it has been observed that many of these models tend to break down under certain environmental conditions, especially during midday periods, when incoming radiation is at a peak. The standard solutions to the heat flow equations are frequently unable to describe the temperature fluctuations to an acceptable accuracy, especially when either the input observation or the calculated value is at or near the surface. The near-surface energy balance is not well described in the above mentioned models, causing significant systematic errors in the temperature calculations.

[6] A simple, physically-based model that can calculate relatively accurate near-surface ($\sim$0–5 cm) soil temperature profiles from a single observation can be a useful tool for many environmental modeling applications. Satellite sensor systems such as AMSR-E, MODIS, ENVISAT-AATSR, TRMM-TMI, and SSM/I, provide spatially distributed land surface temperature products over most of the Earth. This study proposes an approach to model near-surface soil temperature profiles in a bare soil, using only a single temperature measurement, net radiation, and an estimate of the soil moisture content. Two experimental data sets with near-surface temperature measurements within the first centimeter of the soil were used in developing this model. Temperature profiles derived by applying this model to various satellite products may be an important contribution to global energy and water balance studies.

2. Background and Theory

[7] Temperature changes in the soil are essentially driven by the radiative balance, the sum of net short wave solar radiation and net long wave thermal radiation directed toward the soil surface. This net radiation flux is distributed over 1) sensible heat from the surface into the air that is driven by the advection of turbulent air above the surface, 2) latent heat when it is used to vaporize water, and finally 3) the ground heat flux, the conduction of heat vertically through the soil column itself. Continuity of the energy fluxes across the surface is given by:

$$R_N = H + LE + G \tag{1}$$

where R_N is the net radiation, H is the sensible heat flux, LE is the latent heat flux, and G is the soil heat flux. All components are given in W/m^2, R_N and G are positive when directed downward, and H and LE negative. It is important to note that in Equation 1, R_N, LE, and H refer to quantities at the upper (air) side of the air-ground interface, and that they are non-existent or zero at its lower (ground) side. The opposite is true for G. Moreover, energy storage in "the surface" is assumed absent. For a true surface in the mathematical sense - that is, a layer of zero thickness - the latter requirement is definitely met and Equation 1 should conveniently describe G at infinitely small distance below the air-ground interface. Here, we use a different perspective, considering that latent and to a lesser extent also sensible heat fluxes may decrease to zero over a small but finite distance below the land surface. In this approach, G in Equation 1 refers to the ground heat flux density at the depth a [m] below the surface where these fluxes have become negligible. Note that we further must assume that energy storage in the layer is small in comparison with the fluxes, which is reasonable as long as the layer thickness is small. Our approach can be expressed mathematically by rewriting Equation 1 as follows

$$R_N = \int_0^a h(z)\delta z + \int_0^a le(z)\delta z + G(a) \tag{2}$$

where $h(z)$ [W/m^3] and $le(z)$ [W/m^3] denote sensible and latent heat production, respectively. Applying energy balance principles to layers extending from the ground surface to any depth within this boundary zone (that is, $z < a$) yields a more general expression

$$R_N = \int_0^z h(z')\delta z' + \int_0^z le(z')\delta z' + G(z) \tag{3}$$

[8] Equation 3 suggests that within the boundary zone, G is only controlled by latent and sensible heat production above the depth of interest. Hence in the limit, at an infinitely small depth beneath a bare surface, above which no soil air can be exchanged with the atmosphere and no water is present to change phase, soil heat flux may be readily approximated to be equal to net radiation. The relative distribution of the flux rates within the soil is largely determined by the physical properties of the soil medium, e.g., soil particle density, porosity, and especially soil moisture content. The soil column that is influenced by the advective loss of heat through H is assumed to be very shallow, on the order of 1 or 2 millimeters. On the other hand, the depth up to which the soil column is influenced by LE can be much deeper, and can easily extend to 5 cm below the surface for dry soils. Some authors report significant contribution of LE in soil layers at depths of 7 to 10 cm [*Cahill and Parlange*, 1998].

[9] This brings the process of LE generation well into the domain of the soil column that we are interested in when we try to describe differences in temperature at depths between 0 and 5 cm. In this boundary zone where evaporation takes place (but no sensible heat loss to the air), the change in temperature T [K] over time t [s] can be described as:

$$\frac{\partial T}{\partial t} = \frac{\partial}{\partial z} K \frac{\partial T}{\partial z} + E_r(z) \frac{\rho_{lw} L}{(\rho c)_{bulk}} \qquad for\ z < a \tag{4}$$

The first term on the right-hand side is due to Fourier heat conduction with the thermal diffusivity K [m^2/s] and depth z [m]. The second term describes the latent energy loss at source (le in Equation 3), with the evaporation rate $E_r(z)$ [1/s], the density of liquid water ρ_{lw} [kg/m^3] times the latent heat of vaporization L [J/kg] and divided by the bulk heat capacity $(\rho c)_{bulk}$ [J/m^3/K] of the soil/water mixture. This formula assumes that the energy leaves the soil profile at the point where it is used to change the phase of water. The process of condensation of water is included in $E_r(z)$ as a negative evaporation rate. We do not consider the heat that is transported with moisture, nor re-condensation in the soil of vaporized water at a different depth.

[10] At depth a below the surface, also the evaporation rate E_r becomes zero and the heat is distributed only by means of conduction. Below this depth, the change in

temperature over a given interval is governed only by heat conduction. Equation 4 can now be simplified to:

$$\frac{\partial T}{\partial t} = \frac{\partial}{\partial z} K \frac{\partial T}{\partial z} \qquad for\ z \geq a \tag{5}$$

[11] In many empirical approaches to numerical modeling of the soil temperature profile, latent heat loss below the surface is not considered. These approaches are based on Equation 5, and have proven to work well for deeper soil layers. An early example of such a method, and the basis for many later methods, is the solution to the heat flow equations developed by *Van Wijk and De Vries* [1963].

[12] *Van Wijk and De Vries* [1963] describe the diurnal and seasonal variations in soil temperature by sine waves, varying around an average temperature, T_a [K]. T_a is considered constant with depth, due to the assumption of heat conservation. Under normal conditions, the amplitude of the temperature wave is at a maximum at the soil surface and decreases with depth. The maximum temperature also occurs shortly after solar noon at the surface, but lags in time with increasing depth. On the basis of these assumptions, the solution to the heat flow equations for the diurnal cycle is given as [*van Wijk and De Vries*, 1963]

$$T(z,t) = T_a + A \cdot \exp(-z/D) \cdot \sin(\omega t - z/D + \varphi) \tag{6}$$

$$D = \sqrt{2K/\omega} \tag{7}$$

$$\omega = 2\pi/\tau \tag{8}$$

where A [K] is the amplitude of the daily surface temperature fluctuations, t [s] is the time, z [m] is the depth (positive downward), and φ is a phase constant. The damping depth, D [m], is the depth at which the amplitude of surface temperature oscillations is reduced by e^{-1} and is described by Equation 7. The thermal diffusivity is assumed to be constant with depth and time. Finally, the angular frequency ω [1/s], is given as a function of the period of the wave τ [s]. The same approach can be applied to the seasonal temperature cycle in the soil, but for shallow depths ($z <$ 10 cm) the seasonal oscillations are insignificant compared to the diurnal oscillations.

3. Field Observations

[13] Soil temperature, soil moisture, ground heat flux, and radiation measurements from two experimental field studies were used in this study. The first data set is from the U.S. Department of Agriculture Water Conservation Laboratory in Phoenix, Arizona, USA. These data were collected during a three-week dry-down experiment on a loam soil in 1971 [*Jackson*, 1973; *Idso et al.*, 1975]. The second data set was obtained during an 8 month field experiment conducted on a clay soil at the Wageningen Agricultural University meteorological station in Wageningen, Netherlands [*De Jeu et al.*, 2003, www.met.wau.nl]. Both experiments measured soil temperature and moisture at multiple points within the surface profile, with the shallowest near-surface observation within the first centimeter. Measurements were made at 30 minute intervals in each case. These data were supplemented with net radiation and ground heat flux measurements. At the Phoenix site the ground heat flux was measured at 5 cm depth, at the Wageningen site at 2 cm depth. The Phoenix data set has a higher vertical resolution of temperature and moisture measurements than the Wageningen data set, and therefore it was chosen as the calibration data set. The Wageningen data are used to validate the model's performance under somewhat different soil and environmental conditions.

4. Modeling Approach

[14] First we test if the commonly used solutions to conductive heatflow can be applied to temperature oscillations within the first centimeters of the soil column. For this Model A we implement the Van Wijk solutions to the heatflow equations as described in Section 2. We will show where this model breaks down, and explore what the underlying assumptions imply for the ground flux profile. On the basis of these results, a new Model B is proposed, that is specifically designed for the energy transition zone. The performance of this model is tested and compared with Model A.

4.1. Model A

4.1.1. Methods

[15] The Van Wijk heatflow equations (Equations 6–8) can be used to model soil temperature at a depth z_1, from a temperature measured at a depth z_0 and time t_0. From temperature observations with a temporal resolution of 30 min, the 24 h moving average temperature T_{am} is calculated. The diurnal temperature departures from the moving average, $\partial T_D(z_0, t_0)$, described by the sine function in Equation 6 is then given by

$$\partial \mathrm{T}_D(z_0, t_0) = \mathrm{T}(z_0, t_0) - \mathrm{T}_{am} \tag{9}$$

[16] The temperature at depth z_1 can now be modeled by correcting the $\partial T_D(z_0, t_0)$ for the exponential change in amplitude with depth:

$$\mathrm{T}(z_1, t_1) = T_{am} + \partial \mathrm{T}_D(z_0, t_0) \cdot \exp\left(\frac{z_0 - z_1}{D(t_0)}\right) \tag{10}$$

[17] Because of the phase shift of the diurnal temperature cycle between two depths, this model does not calculate the temperature for the same time, t_0, as the initial observation. The time, t_1, is subsequently given by

$$t_1 = t_0 - \frac{z_0 - z_1}{D(t_0)/\omega} \tag{11}$$

This means that t_1 is earlier than t_0 if $z_1 < z_0$, and later if $z_1 > z_0$. However, if the temporal resolution of the measurements is at least one hour, then the calculated temperature can be interpolated accurately at the original observation time.

[18] The damping depth, $D(t_0)$, is calculated according to Equation 7. The diffusivity, K, is calculated from soil properties and the water content θ (m^3/m^3) [*Johansen*, 1975; *Peters-Lidard et al.*, 1998]. This makes the damping depth variable with time (and depth if profile data are

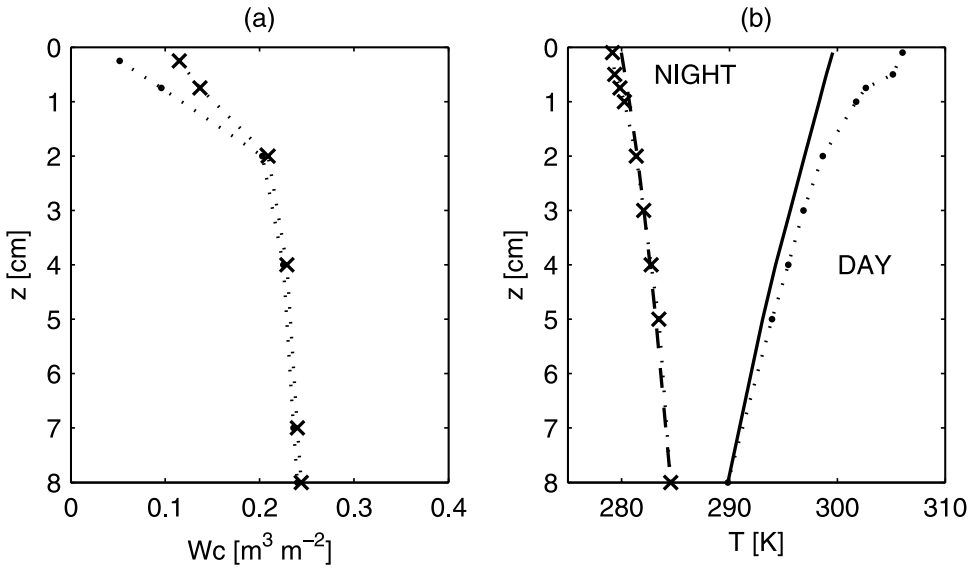

Figure 1. Measured soil moisture and temperature profiles from the Phoenix field experiment at 0100 hours (x) and 1300 hours (.). (a) soil moisture profiles, and (b) measured and modeled temperature profiles. The modeled temperature profiles (heavy lines), are derived from 8 cm temperature observations according to Model A.

available). Ideally, water content should be available at several depths within the first centimeters, so that the soil moisture profile is sufficiently represented. When soil moisture profile data are lacking, it is important that the average soil moisture is reasonably approximated. In this study, the observed soil moisture profile was used to calculate the diffusivity for each layer with temperature measurements.

4.1.2. Results

[19] The Phoenix data set has a relatively dense vertical network of moisture and temperature measurements in the surface profile, and is used to test Model A. Model simulations were performed for 0100 h and 1300 h, as these time periods represent two widely differing conditions; a relatively uniform temperature profile and a warming profile during the period of near-peak solar radiation. Soil moisture profiles for these time periods are also provided to assist in the interpretation of the results (Figure 1a). While some drying is observed in the upper profile during the day, the moisture profiles are essentially the same below 2 cm. The simulated temperature profiles are derived from 8 cm input temperature observations and compared to the measured values (Figure 1b). Model simulations for the nighttime data are seen to correspond well with the observations over the entire profile. However, model simulations during midday clearly underestimate the observations. Although the simulations compare reasonably well to observations within the first several cm of the input value, the difference becomes increasingly larger as one approaches the soil surface.

[20] These results are further supported when we examine several four day time series of diurnal temperature measurements and simulations at different depths (Figure 2). Each plot shows an input temperature, modeled temperature, and the observation at the modeled depth.

[21] Results of upward model simulations (where z_0 = 8 cm and z_1 = 5 cm) and downward simulations (where z_0 = 5 cm and z_1 = 8 cm) are illustrated (Figures 2a and 2b). These time series simulations compare well with observations during the four-day period. RMS errors of 0.6 K and 0.5 K were found for the full diurnal 14-day period, with the RMS errors for the time of greatest daily deviation ($\sim$1300 hours) only marginally higher. However, model simulations from 5 cm to 0.1 cm and 0.1 cm to 5 cm (Figures 2c and 2d) illustrate conditions which result in a breakdown in model performance. In the upward simulation, the modeled temperature underestimates the observation by as much as 10 K during midday, while in the downward simulation the modeled temperature overestimates by as much as 6 K. RMS errors for the full diurnal 14-day period are 3.8 K and 2.5 K respectively, while the RMS errors for the simulations at 1300 hours are 7.9 K and 4.2 K.

4.1.3. Discussion

[22] The above analysis shows that Model A works reasonably well when both the input and modeled temperature depths are well below the surface (Figures 2a and 2b). However, when the input or output depths are near the surface (Figures 2c and 2d), large discrepancies between measured and modeled temperatures are observed during peak radiation periods, and the measured near-surface temperatures deviate from a harmonic surface temperature forcing. The measured temperatures also show a difference between the daily averages at the various temperature depths between 0 and 5 cm. Incoming radiation during peak mid-day periods, often exceeds the soil's ability to transport heat away from the surface. As a result, the surface layers will subsequently experience an unusually high but temporary increase in temperature.

[23] Model A is a simple implementation of Van Wijks solutions to the heatflow equations. Damping and phase shifts with higher harmonics than the daily cycle are not accounted for. This could be improved for shallow depths by adding harmonics that account for higher frequency signals. However, this would not affect the daily averages, and therefore can not describe the measured temperature

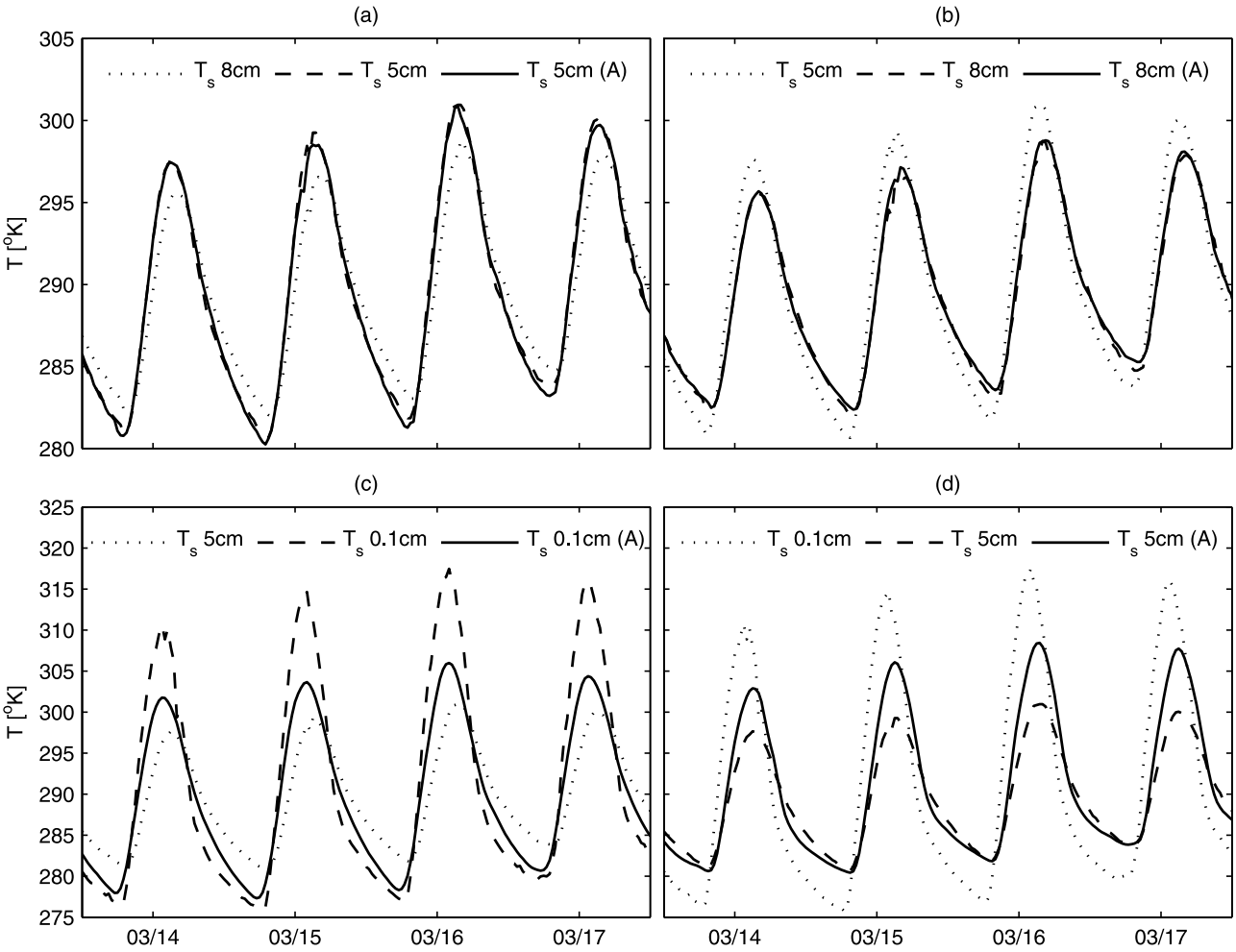

Figure 2. Time series of measured and simulated soil temperatures for four days in March from the Phoenix field data. The solid lines illustrate the modeled temperature according to Model A, the dotted lines show the observed input temperatures, while dashed lines show the observed temperature at the output depth.

time series. These results show that conduction theory is not sufficient in the shallow soil layer and points at the presence of a net heat sink between measurement depths during the observation period.

4.2. Ground Heat Flux

[24] In order to properly describe the temperature changes in the near surface soil layer, one must account for the redistribution of fluxes in the soil, as described by Equation 4. First we will test the assumption that G approaches R_N at the soil surface. The ground heat flux can be calculated between every two consecutive soil temperature values in the vertical profile according to Fourier's Law:

$$G(z) = -\lambda(z) \cdot \frac{\partial T}{\partial z} \tag{12}$$

where λ [W/m/K] is the soil thermal conductivity. The conductivity is calculated with uniform soil properties and profile soil moisture content. The steep temperature gradient observed during the day corresponds to an equally strong gradient in G (Figure 3). When calculating G across small intervals, it is important to record the depths, and consequently δz, with maximum accuracy. It is extremely difficult to maintain constant and accurate instrument depths, especially near the soil surface. This becomes even more problematic when the dimensions of the individual sensor exceed the depth interval between sensors. A difference in the recorded depth of one of the temperature measurements by as little as one millimeter can result in a significant change in the calculated soil heat flux. This, in part, results in the apparent erratic behavior of ground heat flux close to the surface. However, in this paper we hold to the data and recorded depths as originally reported.

[25] Also included in Figure 3 are the measured net radiation, shown at 0 cm, and the measured ground heat flux at 5 cm depth, indicated by '$\diamond$' during the day and 'o' at night. In this example, the measured G(5 cm) underestimates the G as calculated with the gradient method. This is the case for half of the days of the Phoenix experiment. More importantly, it is shown that G approaches R_N close to the surface. Because of the uncertainty in the recording depths, it is difficult to know what shape the G profile really has close to the surface. However, it is clear that the ground flux density approaches the R_N, as predicted from theory. This was found to be the case for every day of the Phoenix

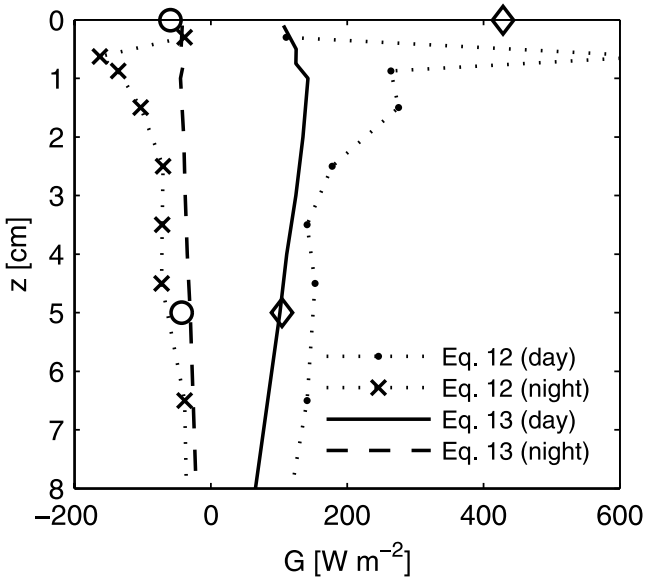

Figure 3. Calculated ground heat flux profiles from measured temperatures gradients at 0100 hours (x) and 1300 hours (•) from the Phoenix field data according to Equation 12. The ground heat flux profiles based on Equation 13 (G_{WB}) are shown as heavy lines. Measured R_N (at 0 cm) and G_{5cm} are indicated by '◇' and 'o' for day and night respectively.

experiment, and in general for the Wageningen data set as well.

[26] *Wang and Bras* [1999] describe a method to obtain the soil heat flux, G_{WB} at any depth from a time series of soil temperature at the same depth. This method is based on Equation 5, and like the Van Wijk approach does not account for possible heat sources or sinks in the soil itself. It states that

$$G_{WB}(z) = \sqrt{\frac{\lambda C_s}{\pi}} \int_0^t \frac{dT(s)}{\sqrt{t-s}} \tag{13}$$

where C_s [J/m^3/K] is the heat capacity of the soil material and s [s] is the integration variable. Equation 13 does not require specific constrains regarding the temperature time series that is used. Figure 3 shows that G_{WB} is very different than the G as calculated with Equation 12. In general G_{WB} has a relatively uniform profile during the day and night. G_{WB} correctly describes the G(5cm), as measured by heat flux plates. Below ~4cm during the day, and ~3cm during the night, both G profiles are uniform, although the magnitude of the fluxes is not the same. This is in accordance with *Cahill and Parlange* [1998], who report a significant contribution (40–60%) to the total heat flux by the vapor flux as low as 7–10 cm, a process not accounted for in Equation 13. Furthermore, G_{WB} increasingly underestimates the ground heat flux closer to the surface during the day, and overestimates the ground heat flux during the night. A similar result is found when the gradient method is applied to the temperature series derived from Model A (not shown). These results are consistent with the previous discussion, where it was stated that the underlying assumptions of the Van Wijk model, and by extension the Wang and Bras method as well, implicitly result in an underestimation of the gradient in ground heat flux density near the surface.

[27] The strong gradient in ground flux density near the surface, and the inability to describe this with pure conductive processes gives evidence of heat sources and sinks below the surface. Secondly, it is shown that indeed the ground flux density approaches R_N at the surface. Both these observations suggest the possibility of modeling the ground heat flux profile in the energy transition zone based only on the net radiation, estimated soil moisture, and an estimate of the ground heat flux at 5 cm. This is explored further in the next section.

4.3. Model B

[28] As shown previously, Model A is not able to describe the near surface temperature fluctuations during periods of high incoming radiation. Another drawback in applying Model A is the need for a sufficient number of consecutive temperature measurements that typically are not available at satellite temporal scales. For these reasons a new approach is proposed that is better able to describe the near surface temperatures. The first step consists of generalizing the shape of the instantaneous ground heat flux profile relative to net radiation and the ground heat flux at 5 cm. In the second step, this modeled ground flux profile is used together with the moisture content of the profile to extrapolate the temperature from a single observation depth to a complete surface temperature profile. Because the instantaneous ground heat flux is modeled, no phase correction is needed, making this approach ideally suited for satellite applications that have limited temporal resolution.

4.3.1. Method

[29] As described in the previous section, the ground heat flux can be calculated between any two temperature measurements in the vertical profile. From the temperature observations from both the Phoenix and Wageningen field experiments it was found that the shape of the ground heat flux profile can be generalized relative to R_N and an estimated ground heat flux at 5 cm during the day. From theory and field data we know that G approaches R_N at the surface and that below a certain depth, G continues to decrease only slowly with depth (see Figure 3 day). If the loss terms LE and H are distributed over the energy transition zone in a bell shaped form (a sine function from 0 to π), then the shape of the flux density, $S(z)$, is the derivative of the loss function, a cosine function with the opposite sign. Choosing the parameters so that $S = 1$ at the surface and $S = 0$ at $z = \alpha$, the shape of the ground heat flux profile can be described as:

$$S(\mathrm{z}) = 0.5 \cdot \cos(\pi \cdot \mathrm{z}/\alpha) + 0.5 \tag{14}$$

where α is the lower boundary depth of the energy transition zone, defined as the depth up to which partitioning of energy takes place over H, LE and G. The depth α is strongly related to the moisture content, and in our data sets, values of α are found between 2 and 5 cm. The ground heat flux can then be expressed as:

$$\mathrm{G(z)} = \mathrm{R_N} \cdot (\beta + (1-\beta) \cdot S) \textit{ for daytime} \tag{15}$$

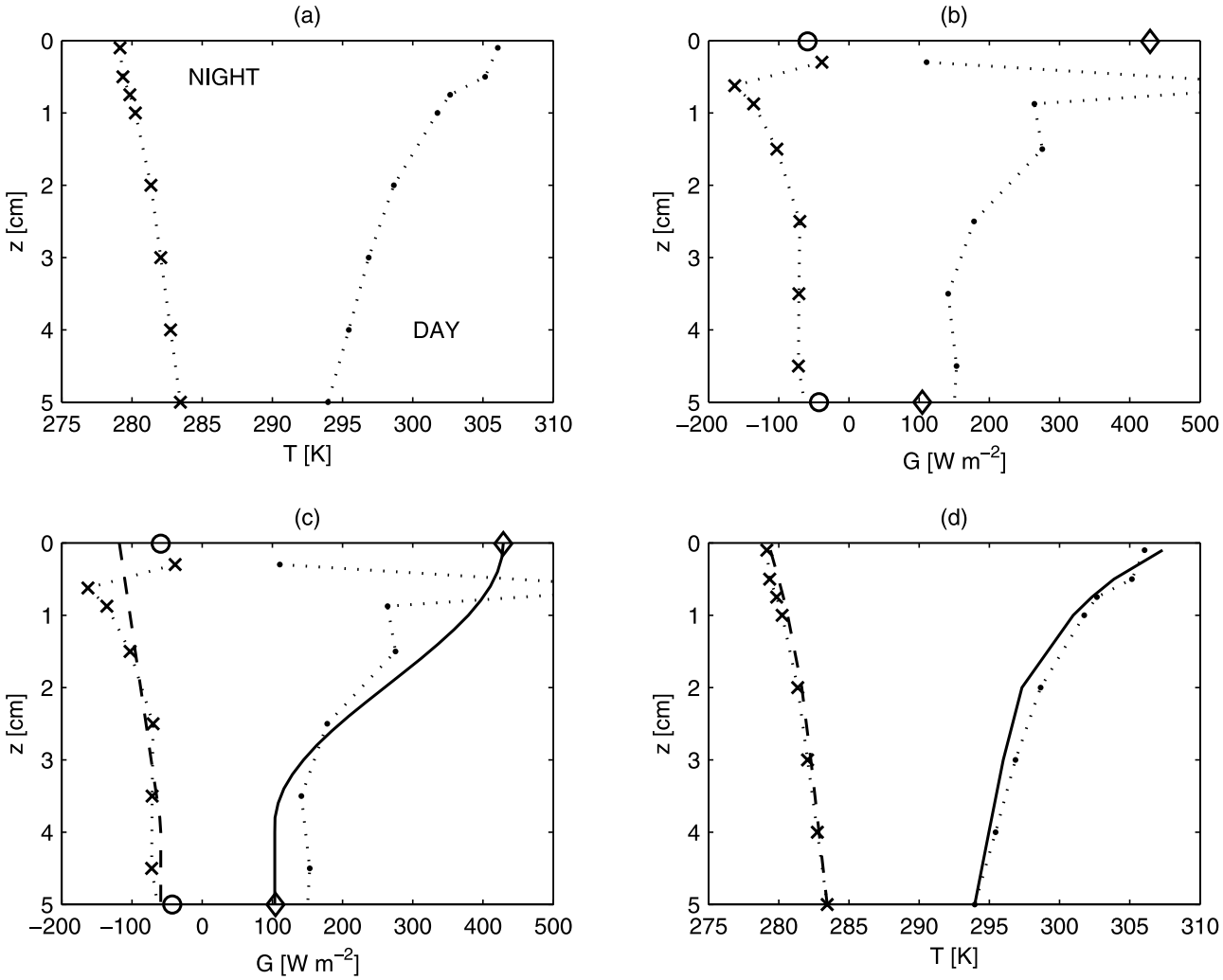

Figure 4. (a) Measured temperature profiles from the Phoenix field data, at 0100 (x) and 1300 (●) hours; (b) Ground heat flux profile as calculated from the observed temperature profiles as shown in (a); Measured R_N and G_{5cm} are indicated by '◇' and 'o' for day and night respectively. (c) Modeled ground heat flux profile (heavy lines), compared with G profile derived from temperature observations. (d) Modeled temperature profiles (heavy lines) derived from the modeled G profiles, and compared with observations.

where β is the ratio of G_{5cm}/R_N during the day. If the ratio G_{5cm}/R_N is unknown, it can be estimated at approximately ~0.25. This is slightly less than the average value for the entire day of ~0.3 as found in the literature (*Fuchs and Hadas*, 1972; *Idso et al.*, 1975; *Kustas and Daughtry*, 1990), where the ground heat flux was measured at shallower depths.

[30] At night, the soil surface loses heat to the atmosphere instead of gaining heat from incoming radiation. The R_N at night does not drive the ground heat flux, but rather is a result of it. Also different processes, such as dew, come into play at night. It is therefore not surprising that the G profile has a different relation with R_N at night. This is shown for the Phoenix field data (see Figure 3 night), where it was found that the nighttime G profile starts at approximately 1.5 times the R_N at the surface to approximately equal to the R_N at a depth of $z = a$:

$$G(z) = R_N \cdot (1 + 0.5 \cdot S(z)) \text{ for nighttime} \quad (16)$$

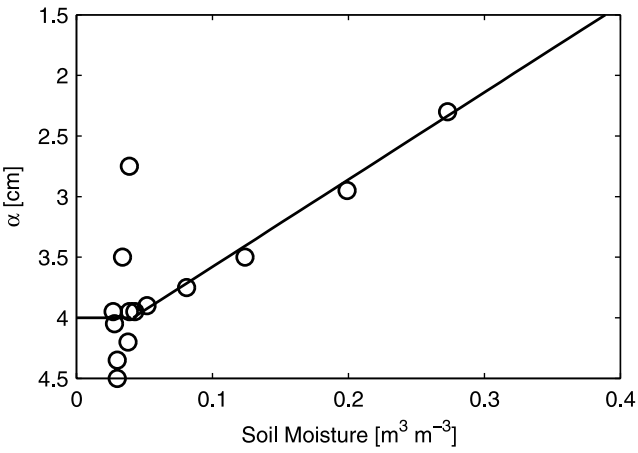

Figure 5. Optimized values of α for each day of the Phoenix experiment, as a function of the 1300 hour soil water content at 0.25 cm.

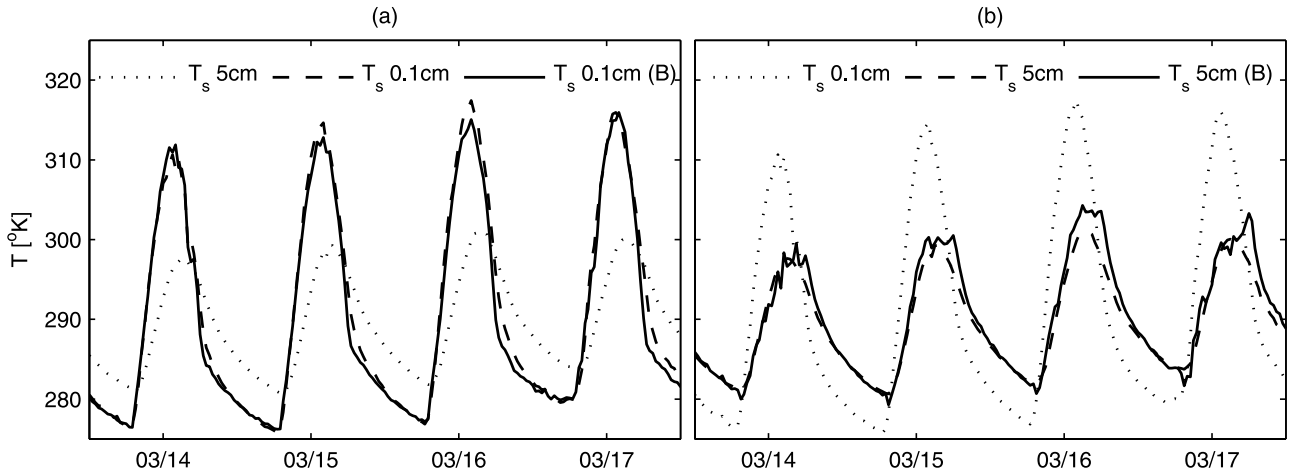

Figure 6. Four-day time series of measured and simulated soil temperatures from the Phoenix field experiment. The solid lines indicate the modeled temperature according to Model B; the dotted lines show the measured input temperatures; dashed lines show the measured temperature at the output depth.

Because the nighttime fluxes are generally lower, the temperature model is less sensitive to the precise shape of the nighttime ground heat flux profile.

[31] With G now approximated, the temperature difference over a soil layer with thickness δz can then be calculated by inverting Equation 12, such that

$$\partial T = G(z) \cdot \partial z / \lambda \tag{17}$$

Because the thermal conductivity is a function of soil moisture content, this step is highly dependant on the moisture profile of the soil column.

4.3.2. Calibration

[32] The depth, α, is dependent on moisture content because it determines the availability of water for evaporation. When the soil moisture content is high, the available energy for evaporation will leave the soil in a relatively shallow soil layer and α will be small. In a soil with dry upper layers, evaporation will take place at lower depths where moisture is available, resulting in a thicker energy transition zone (higher α).

[33] The relationship of α with moisture content is derived from the Phoenix data. The steps for this procedure are outlined in Figure 4. From the measured temperature profile (Figure 4a) we calculate the ground heat flux profile (Figure 4b). Observed values for R_N (shown at 0 cm), and $G_{5\text{cm}}$ are indicated with a diamond (1300 h) and a circle (0100 hours). Next, we model the G profile using observed R_N and $G_{5\text{cm}}$ with Equations 14–16 (Figure 4c). We then recalculate the temperature profile, based on the temperature at 5 cm and the modeled G profile according to Equation 17 (Figure 4d).

[34] The depth α is optimized to yield the lowest RMS error for the modeled temperature profile. While the optimized G profile compares only loosely to the calculated profile (Figure 4c), much of the difference between the two

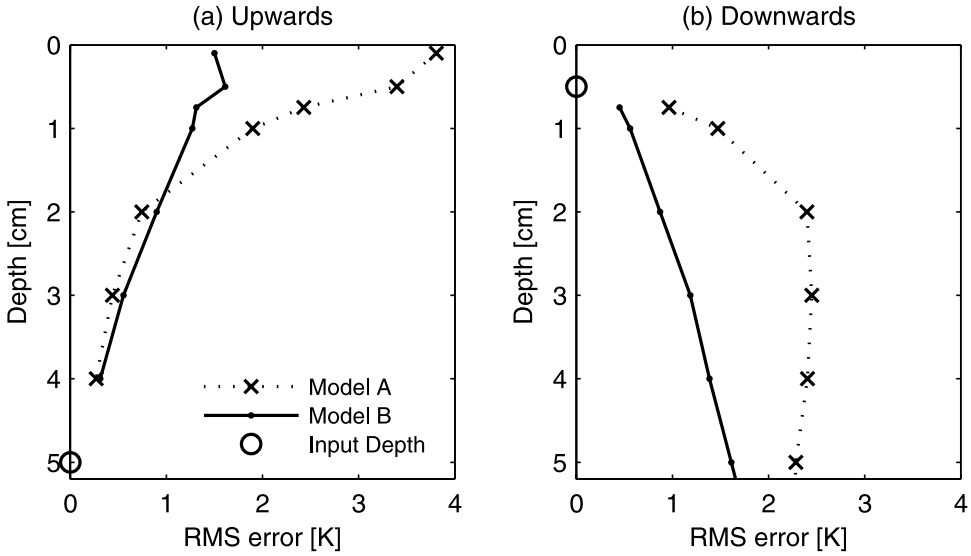

Figure 7. Error profiles comparing performance of models A and B in both upward (z_1 = 5 cm) and downward (z_1 = 0.5) directions.

Table 1. Results for Selected Periods of the 2003 Wageningen Field Experiment[a]

Period	Dates	Avg. Wc, (cm^3/cm^3)	Avg. β(-)	Surface Sensor Depth, (cm)	RMS error [K]			
					Entire Period		At 1300 h	
					A	B	A	B
1	12–18 April	0.2	0.31	0.5	3.6	2.6	5.4	0.5
2	**7–11 May**	**0.37**	**0.29**	**0.5**	**1.8**	**1.0**	**3.4**	**1.0**
3	30 May–4 June	0.32	0.27	0.5	2.5	1.4	5.0	2.8
4	8–15 July	0.06	0.26	0.3	4.2	2.4	8.5	3.2
5	**28 July–3 August**	**0.06**	**0.26**	**0.1**	**6.2**	**2.0**	**11**	**1.5**
6	6–9 August	0.04	0.28	0.1	7.8	2.1	15	3.0
7	15–21 September	0.03	0.36	0.1	6.2	2.6	11	3.1
8	2–5 October	0.09	0.26	0.1	2.2	1.5	2.8	1.9

[a]The RMS error between the measured surface temperature and the modeled value for Model A and B are shown, for both the entire period and for the 1300 hour value. Bold periods are illustrated in Figure 8.

can be accounted for by small variations in the recorded depths, as discussed earlier in Section 4.2. Another possible uncertainty may be in the accuracy of the G_{5cm} measurement and its recorded depth. Nevertheless, the corresponding temperature profile compares well to the measured profile, with an RMS error of 1.2 K (Figure 4d).

[35] The above procedure was repeated for each measurement day, in order to derive values of α for all available soil moisture conditions. Figure 5 shows how these optimized values relate to the soil moisture content (θ) at 0.25 cm. The 0.25 cm depth was chosen because α showed the highest sensitivity to moisture content at this depth. The relationship between α (cm) and moisture content may be described as:

$$\begin{aligned} \alpha &= 4.3 - 7.2 \cdot \theta \qquad for\ \theta \geq 0.04 \\ \alpha &= 4.0 \qquad\qquad\quad for\ \theta < 0.04 \end{aligned} \tag{18}$$

When the soil moisture content is less than 0.04 m^3/m^3, the latent heat flux component is extremely small, and results in a large scatter in the thickness of the energy transition zone (α). For these conditions we set α to 4 cm. When this relationship is applied to soil moisture depths other then 0.25 cm, best results are expected for soil moisture records within the first centimeter of the soil.

4.3.3. Results

[36] The above-approach is applied to the Phoenix field data for the same period illustrated previously in section 4.1.2, using the average value of β for the entire 14-day experimental period and the calibrated value of α. Results of upward model simulations (where z_0 = 5 cm and z_1 = 0.1 cm) and downward simulations (where z_0 = 0.1 cm and z_1 = 5 cm) are illustrated (Figures 6a and 6b). These simulations result in RMS errors of 1.5 K for the full period, which is a significant improvement over the Model A. Likewise, the errors at the time of greatest daily deviation are reduced to 2.1 K.

[37] The performance of Model B is compared to Model A by calculating the errors between measured and simulated temperatures at all modeled depths for which data are available. The output temperatures are modeled with input temperatures of 5 cm (upward modeling) and 0.5 cm (downward modeling). Upward simulations show similar error profiles for both approaches up to about 2 cm with maximum errors of 0.9 K (Figure 7a). Above 2 cm, however, the error profiles diverge considerably, with errors

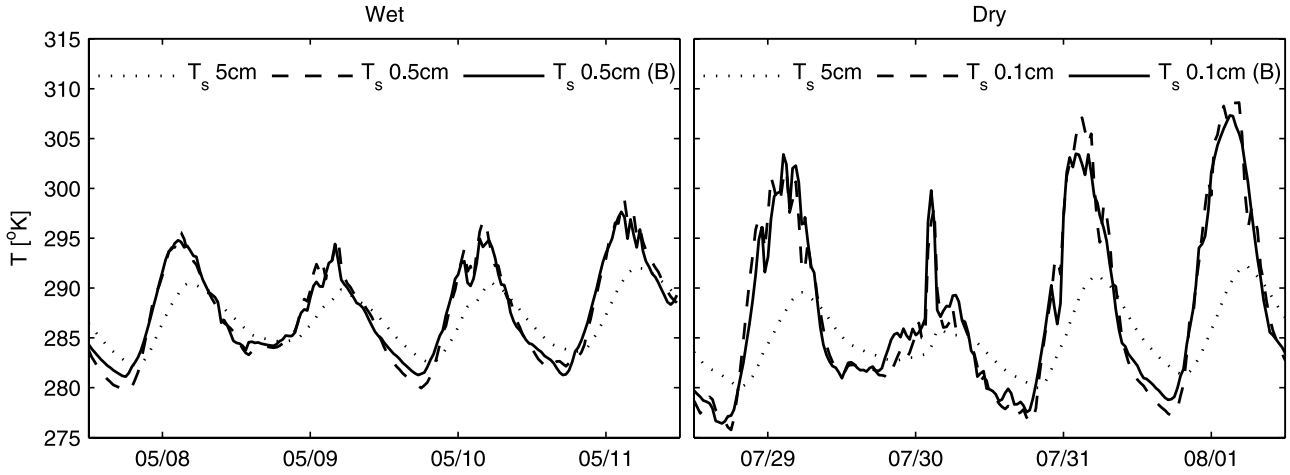

Figure 8. Four–day time series of measured and simulated soil temperatures from the Wageningen field experiment for two periods: one with wet and one with dry conditions. The solid lines indicate the modeled temperature at 0.5 cm (wet) and 0.1 cm (dry) according to Model B; the dotted lines show the measured input temperatures at 5 cm; dashed lines show the observations at the modeled depth.

Table 2. RMS Error [K] for Simulations B0-B3[a]

	Period 2 – Wet				Period 5 – Dry			
	B0	B1	B2	B3	B0	B1	B2	B3
Entire Period	1.0	1.1	1.2	1.3	2.0	2.1	2.3	2.9
1300 h	1.0	1.5	1.75	2.1	1.5	1.4	2.2	3.8

[a]See text for explanation.

at 0.5 cm of 3.4 K for Model A and 1.6 K for Model B. In the downward simulations (Figure 7b), both models show low errors of 0.5 K to 1.0 K at 1 cm. However, Model B errors increase only slightly with depth and are still only 1.6 K at 5 cm, while Model A errors increase more rapidly to a maximum of 2.4 K at 2 cm and remain above 2.2 K down to 5.0 cm.

5. Model Validation

[38] Model validation is performed with the independent Wageningen data set described in Section 3. Eight 5–7 day periods are selected with little or no clouds and precipitation, representing a range of soil moisture contents. In the validation of Model B, the relationship as derived earlier for the α parameter (Equation 18) was used. For the β ratio, the period average 1300 hour value of the G_{2cm}/R_N measurement is used, and varies between 0.25 and 0.35 over the 8 month experimental period. This compares to the Phoenix average value of $\beta = 0.23$.

[39] Table 1 shows the eight selected periods, with average water content, β ratio, surface sensor depth, and RMS errors for models A and B. Model A again performs poorly with RMS errors for the period from 1.8 to 7.8 K, with highest values for the driest periods. Model B performs much better with RMS errors for the period in a more acceptable range from 1.0 to 2.6 K. Highest RMS values are again associated with the driest periods. The most significant improvement in model performance is also seen in the dry periods.

[40] The diurnal time series for a wet 5 day period in May and a dry 7 day period in July/August are illustrated in Figure 8 for the 5 cm to 0.5 cm and 0.1 cm simulations. Both wet and dry time series of modeled temperatures are shown with both the input observations as well as observations at the modeled depth. The RMS error for the full wet period is 1.0 K and for the dry period 2.1 K. The RMS errors for the time of greatest daily deviation are also low with 0.8 K for the wet period and 3.0 K for the dry period. These results give confidence that the new model has validity in a different soil and for a time period that covers meteorological conditions differing from a wet spring to a dry summer and fall.

6. Remote Sensing Application

[41] For global, remote sensing–based applications, site specific β ratios will most likely not be available and a constant value can be used. To test the effect of this generalization, the RMS errors for Model B are calculated using $\beta = 0.25$ as was suggested in section 4.3.1, in a downward simulation using the observed 0.5 cm temperature as the input value to model the temperature at 5 cm. Remotely sensed measurements from microwave observations can provide an average temperature for the top 0.3 cm layer, so using the 0.5 cm value will give reasonable approximation of the errors that can be expected. The results are listed in Table 2, as simulation B1. These values vary only slightly from the values for the corresponding time periods reported in Table 1 (also given as B0 in Table 2). This suggests that Model B is less sensitive to the β ratio and that a value of 0.25 may be a reasonable first approximation for global studies.

[42] Another important limitation in remote sensing applications is that soil moisture profile data will most likely not be available. If retrieved from satellite measurements, soil moisture data will represent the average moisture content of a shallow surface layer ($\sim$1.0 cm at currently available space technology). We test this effect by using the average of the 0.5 cm and 2.0 cm soil moisture measurements (simulation B2). The resulting errors are similar in magnitude to the previous simulation (B1), except for the 1300 h values during the dry period, which are somewhat higher. Further model improvements may be realized with additional experimental data observed under drying surface conditions which may help parameterize moisture profile characteristics from remote sensing observations.

[43] An additional limitation is the accuracy of soil moisture from satellite sensors. The official NASA AMSR-E global soil moisture data set has an estimated accuracy of $\sim$6% (absolute) and represents a surface layer of approximately 1.0 cm [*Njoku*, 2004; *Wagner et al.*, 2007], although recent results from other retrieval algorithms suggest the possibility of improved accuracy. We simulate the effect of possible errors in the soil moisture estimates by adding random noise to the soil moisture data with a standard deviation of 0.06 m^3/m^3. Again, this simulation (B3) shows only a small increase in the error for the wet period, although the dry period is affected somewhat more.

7. Summary and Conclusions

[44] Two field data sets are used to model near-surface soil temperature profiles in a bare soil. It is shown that the commonly used solutions to the heat flow equations by Van Wijk perform well when applied at deeper soil layers, but result in large errors when applied to near surface layers, where more extreme variations in temperature occur during periods of peak incoming radiation. The reason for this is that these approaches do not consider heat sources or sinks below the surface.

[45] An approach, suitable for application with satellite temperature data products is subsequently tested to model instantaneous near-surface soil temperature profiles in a bare soil from a single observation depth. The concept behind this approach is that the magnitude of the ground heat flux approaches net radiation for $z \rightarrow 0$, and that sensible and latent heat fluxes have their source below the surface. The distribution of fluxes over this energy transition zone has to be accounted for to describe the measured near surface temperature profiles. The proposed approach consists of two parts: 1) Deriving an instantaneous soil heat flux profile based on net radiation and the ground heat flux at 5 cm depth; 2) Using this modeled ground heat flux

profile to extrapolate a single temperature observation to a complete near-surface temperature profile. Both steps are sensitive to the soil moisture content of the profile.

[46] Error analysis shows that this approach results in errors that are significantly lower compared to the approach based on Van Wijk's solutions. For the maximum depth of 5 cm between the input and modeled temperature depth, the observed errors for the validation data are between 1 and 3 K. While the errors for the dry periods are on the high side of this range, they are still acceptable for many applications, and indicate that the surface processes are reasonably well described. The validation results also show that the model functions at a range of soil and meteorological conditions. The proposed model is tested under limitations in input data that are associated with remote sensing applications. It is shown that these limitations result in only small increases in the overall error. This approach may be useful for satellite–based global energy balance applications.

[47] **Acknowledgments.** This work was funded in part by the NASA Headquarters Modeling and Prediction Branch and the Vrije Universiteit Amsterdam. The authors would like to thank the Water Conservation Laboratory, Phoenix, AZ for making the Phoenix data available and the Meteorology and Air Quality group of Wageningen Agricultural University for the use of their experimental field site.

References

Camillo, P. (1989), Estimating soil surface temperatures from profile temperature and flux measurements, *Soil Sci.*, *148*, 233–249.

Cahill, A. T., and M. B. Parlange (1998), On water vapor transport in field soils, *Water Resour. Res.*, *34*(4), 731–739.

Cuaraglia, D., J. Pousa, and L. Pilan (2001), Predicting temperature and heat flow in a sandy soil by electrical modeling, *Soil Sci. Soc. Am.*, *65*, 1074–1080.

De Jeu, R., T. Holmes, and M. Owe (2003), Deriving Land Surface Parameters from 3 different vegetated sites with the ELBARA 1.4-GHz Passive Microwave Radiometer, *Proc. SPIE*, *5232*.

Elias, E., R. Chicota, H. Torriani, and Q. de Jong van Lier (2004), Analytical soil-temperature model: Correction for temporal variation of daily amplitude, *Soil Sci. Soc. Am. J.*, *68*, 784–788.

Fuchs, M., and A. Hadas (1972), The heat flux density in a non-homogeneous bare loessial soil, *Boundary Layer Meteorol.*, *3*, 191–200.

Idso, S., J. Aase, and R. Jackson (1975), Net radiation-soil heat flux relations as influenced by soil water content variations, *Boundary Layer Meteorol.*, *9*, 113–122.

Jackson, R. (1973), Diurnal changes in soil water content during drying, in *Field Soil Water Regime*, edited by R. R. Bruce et al., special pub. 5. Madison, WI, *Soil Sci. Soc. Amer. Proc.*, *5*, 37–55.

Johansen, O. (1975), Thermal conductivity of soils, Ph.D thesis, University of Trondheim, p. 236.

Kustas, W., and C. Daughtry (1990), Estimation of the soil heat flux/net radiation ratio from spectral data, *Agric. For. Meteorol.*, *49*, 205–223.

Njoku, E. (2004), updated daily, AMSR-E/Aqua Daily L3 Surface Soil Moisture, V001, *National Snow and Ice Data Center*, Boulder, CO, USA. Digital Medi.

Peters-Lidard, C. D., E. Blackburn, X. Liang, and E. F. Wood (1998), The effect of soil thermal conductivity parameterization on surface energy fluxes and temperatures, *J. Atmos. Sci.*, *55*, 1209–1224.

Wagner, W., V. Naeimi, K. Scipal, R. de Jeu, and J. Martínez-Fernández (2007), Soil moisture from operational meteorological satellites, *Hydrogeol. J.*, *15*, 121–131.

Wang, J., and R. L. Bras (1999), Ground heat flux estimated from surface soil temperature, *J. Hydrol.*, *216*, 214–226.

Van Wijk, W. and D. de Vries (1963), Periodic temperature variations in a homogeneous soil, in *Physics of plant environment*, edited by W. R. Van Wijk, North-Holland Publ. Co., Amsterdam, pp. 102–143.

R. H. M. De Jeu, T. R. H. Holmes, and H. Kooi, VU University Amsterdam, Dept. of Geo-Environmental Sciences, De Boelelaan 1085, 1081 HV, Amsterdam, The Netherlands. (thomas.holmes@falw.vu.ul)

M. Owe, NASA GSFC, Hydrological Sciences Branch, Code 614.3, Greenbelt Rd, Greenbelt, MD 20771, USA. (manfred.owe@nasa.gov)